J. Synchrotron Rad. (1998). **5**, 1133–1135

Phase-contrast X-ray CT image of breast tumor

Tohoru Takeda,[a]* Atsushi Momose,[b] Ei Ueno[a] and Yuji Itai[a]

[a]*Institute of Clinical Medicine, University of Tsukuba, 1-1-1 Tennodai, Tsukuba-shi, Ibaraki 305-8575, Japan, and* [b]*Advanced Research Laboratory, Hitachi Ltd, Hatoyama, Saitama 350-0321, Japan. E-mail: ttakeda@md.tsukuba.ac.jp*

(*Received 4 August 1997; accepted 22 December 1997*)

Phase-contrast X-ray CT images generated by differences in refractive indices can be used to visualize the internal structures of soft tissues without contrast enhancement. In this study, imaging of human breast tumor was performed on formalin-fixed samples. Experiments were carried out at the synchrotron source of the Photon Factory, Tsukuba, Japan. The X-ray energy was adjusted to 17.7 keV. Phase-contrast X-ray CT images revealed various structures of human breast tumor as clearly as optical images.

Keywords: phase-contrast X-ray CT; breast tumor; optical image; interferometer.

1. Introduction

Present clinical X-ray images are generated by differences in linear attenuation coefficients. However, discrimination between tumorous lesions and normal tissues is difficult because the difference in the linear attenuation coefficient is below the detection limit. However, phase-contrast X-ray images, which are generated by differences in the refractive indices, have a great potential for demonstrating the structures inside soft tissues without contrast enhancement because about 1000 times higher sensitivity is obtained compared to that of the conventional absorption method (Momose & Fukuda, 1995).

Phase-contrast radiograms using an X-ray interferometer (Bonse & Hart, 1965; Hart, 1975) have been used to image various structures within biological objects such as bone (Ando & Hosoya, 1972), cerebellum (Momose & Fukuda, 1995) and metastatic tumor (Takeda *et al.*, 1995). The image of bone was obtained using an X-ray tube, whereas other images were obtained by using a synchrotron X-ray source. Phase-contrast X-ray CT (Momose, 1995) clearly demonstrated rabbit cancer lesions (Momose, Takeda & Itai, 1995; Momose *et al.*, 1996*a*,*b*), human pathological specimens (Momose, Takeda, Itai & Hirano, 1997; Momose, Takeda & Itai, 1998; Takeda *et al.*, 1998) and rat cerebrum (Bonse & Busch, 1996; Beckmann *et al.*, 1997). In this paper, a comparison between a phase-contrast X-ray CT image and an optical image of a human breast tumor is reported.

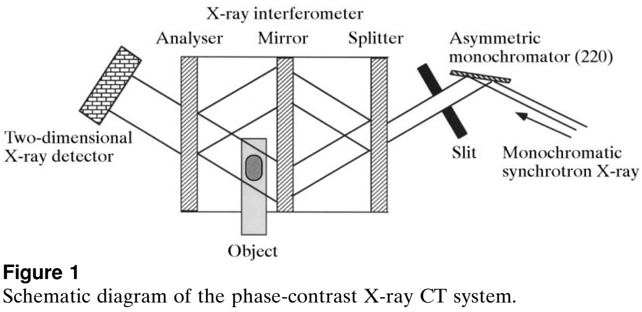

Figure 1
Schematic diagram of the phase-contrast X-ray CT system.

2. Methods and materials

Experiments were performed at the three-pole superconducting vertical wiggler beamline BL-14B of the Photon Factory, Tsukuba, Japan. Phase-contrast X-ray CT consisted of an asymmetric silicon crystal (220), a triple Laue-case X-ray interferometer [silicon (220)] and an X-ray detector system (Suzuki *et al.*, 1989) (Fig. 1). The X-ray interferometer, which was made from a large and

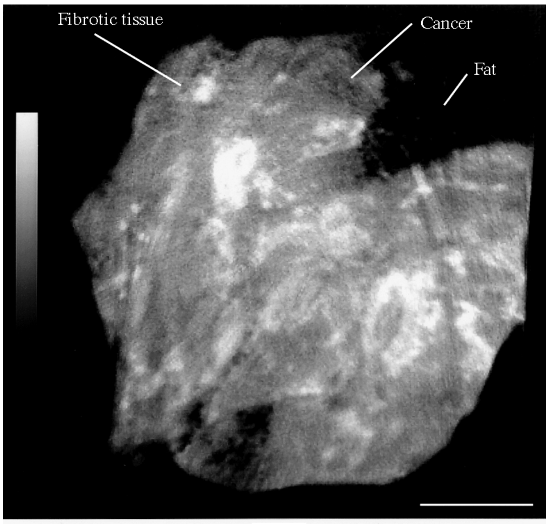

(*a*)

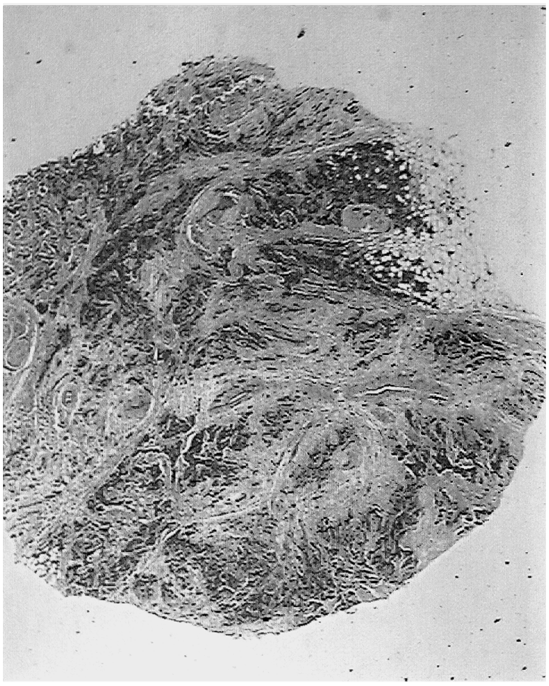

(*b*)

Figure 2
Breast cancer. (*a*) Phase-contrast X-ray CT image. (*b*) Optical image; a part of the pathological sample was out of view.

highly perfect single-crystal block by cutting two wide grooves in the block, had three parallel X-ray half mirrors called beam splitter, mirror and analyser. Using symmetrical Laue diffraction in the beam splitter, the incident radiation is divided into two coherent beams. These beams become spatially separated before they reach the mirror, where they are again reflected in the Laue case and overlap at the entrance surface of the analyser. Here, the beams set up an interference pattern (Bonse & Hart, 1965). The X-ray energy was set to 17.7 keV by the monochromator and the X-ray flux ahead of the object was estimated at about 5×10^5 photons $mm^{-2}\,s^{-1}$. The typical beam current was 350 mA at 2.5 GeV.

The specimens were pathological human breast lesions such as breast cancer fixed in formalin. The breast cancer lesions were obtained from the center of a large cancer specimen. The specimen was inserted in the object beam path between the mirror and the analyser of the interferometer. This specimen was rotated against the object beam. Image aquisition time for phase-contrast X-ray CT was 60 s $projection^{-1}$. Phase-contrast X-ray CT images were obtained at $(12)^3$ μm^3 voxel and the field of view was 5×5 mm.

3. Results

Though this system restricted the field of view to 5×5 mm, the phase-contrast X-ray CT image clearly demonstrated various structures within human pathological specimens such as breast cancer.

The viable breast cancer area appeared violet on the optical image and was described as dark by phase-contrast X-ray CT (Fig. 2). Dense fibrotic tissues within the cancer lesion were shown as white linear and band-like structures; however, rough fibrotic tissues were shown as slightly dark. Fat tissues were represented as a black wedge area.

Normal breast tissue (Fig. 3) constructed of dense fibrotic tissue demonstrated a bright contrast. The surrounding rough fibrotic tissues were shown as a moderately dark area and the various

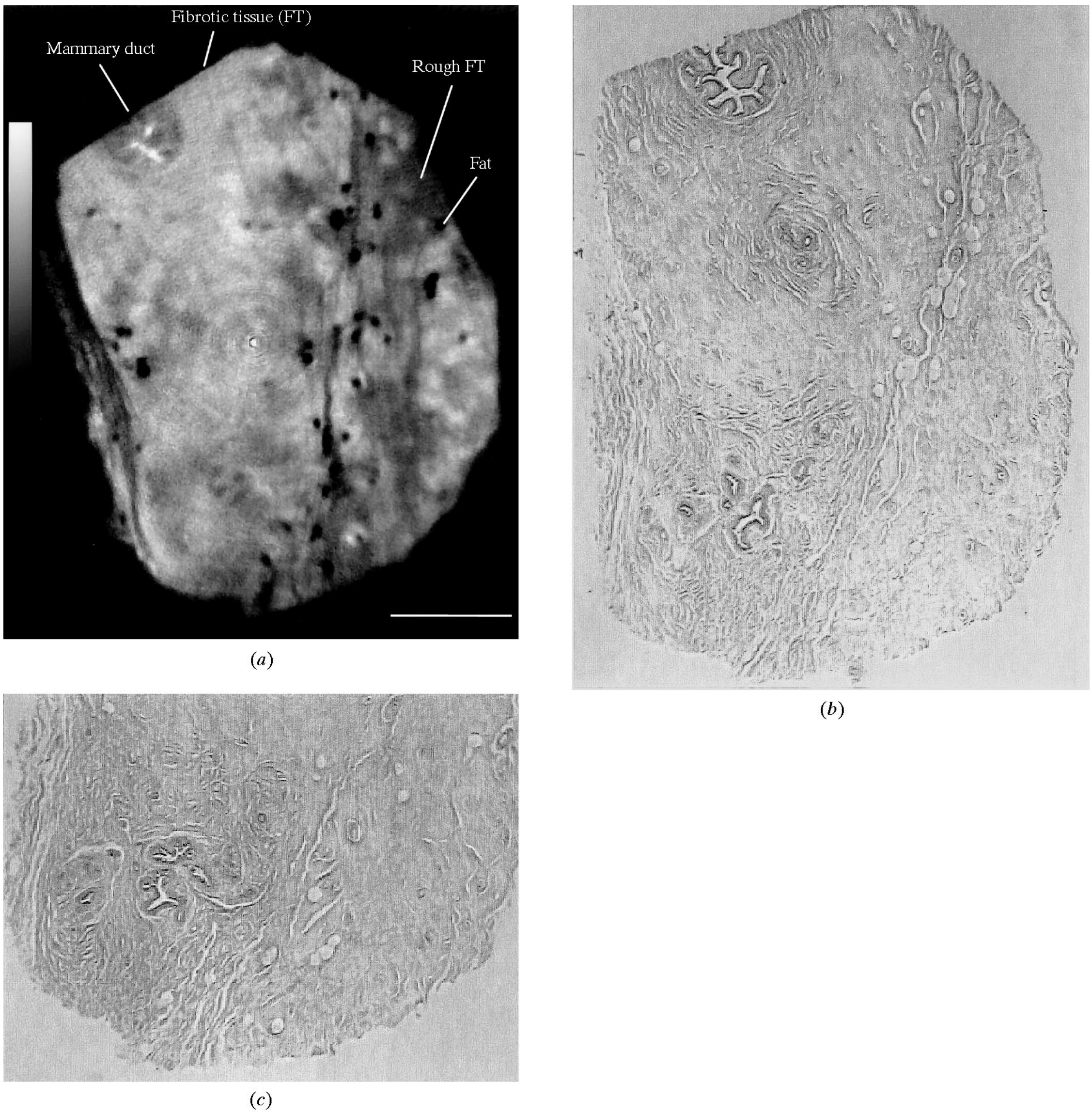

(*a*)

(*b*)

(*c*)

Figure 3
Normal breast tissue. (*a*) Phase-contrast X-ray CT image. (*b*), (*c*) Optical image. As the cut slice of the pathological specimen was oblique and not flat, the slice most nearly corresponding to the image was described. (*c*) Upper portion of pathological sample.

shapes of voids were adipose tissues. The fibroglandular tissue and mammary ducts with dense epithelial cells were surrounded by the rough fibrotic tissue. These images were shown as tree-like white branches surrounded by a dark area. These pathological specimens did not contain calcified lesions.

4. Discussion

4.1. *Significance of phase-contrast X-ray images of breast tumor*

Without contrast enhancement, the image of phase-contrast X-ray CT revealed various soft-tissue structures in breast specimens such as fat tissue, fibrosis, cancer lesions and ducts quite similar to those shown on optical images. Phase-contrast X-ray CT could detect the X-ray diffractive index corresponding to the density of the object (Momose *et al.*, 1996*a*,*b*). The area displayed as white corresponds to lesions with high density, whereas the area displayed as dark has a low density. Fat tissues show a significantly lower density as established by conventional X-ray CT. Cancer regions also have a low density. Fibrous tissue varies in density owing to the roughness of fibrotic fiber networks. The present specimens did not contain the microcalcification 'Psammoma body', which is clinically used as one of the important signs in diagnosing malignancy of breast tumor by mammography. However, these preliminary experiments indicated that phase-contrast imaging had an excellent ability to differentiate various soft-tissue structures of breast lesions even without demonstrating microcalcification. Further imaging studies should be performed to clarify the clinical significance but phase-contrast imaging might allow more detailed diagnosis of breast tumor than conventional X-ray imaging.

4.2. *Present limitations and future improvements*

The spatial resolution of phase-contrast X-ray CT is now about 30 μm (Momose *et al.*, 1996*b*), which is insufficient for detailed diagnosis of pathological structures with the same precision as optical microscopic images. As the size of cells is about 10 μm, the present phase-contrast X-ray images provide an averaged image of various cells and interstitial structures. The fine pathological structures disappeared but spatial resolution of the image, which is thought to be quite similar to those by optical loupe, could not be obtained by conventional X-ray imaging. The spatial resolution of images might be improved by faster image aquisition than the present experiment (about 8 h) using a high-flux X-ray source.

The field of view in this experiment was very small, 5×5 mm, so a resected pathological specimen was used for observation. An experiment with a live animal or intact organ could not be performed using the present system. To increase the field of view for imaging larger samples, a separate type of interferometer (Becker & Bonse, 1974; Momose, Yoneyama & Hirano, 1997; Momose, Takeda & Itai, 1997; Momose, Takeda, Itai, Yoneyama & Hirano, 1998) or a larger triple-Laue-case (L–L–L) X-ray interferometer must be fabricated.

5. Conclusions

Imaging of breast tumor could be performed by phase-contrast X-ray CT with synchrotron radiation. Various structures of breast lesions were described almost as clearly as with an optical loupe. Further improvements to expand observation size and *in vivo* inspection are planned

This research was partially supported by a Grant-in-Aid for Scientific Research No. 08407024 from the Japanese Ministry of Education, Science and Culture. Experiments were performed under proposal No. 95 G349 approved by the National Laboratory for High Energy Physics.

References

Ando, M. & Hosoya, S. (1972). *X-ray Phase-Contrast Microscopy*, edited by G. Shinoda, K. Kohra & T. Ichikawa, pp. 63–68. University of Tokyo Press.

Becker, P. & Bonse, U. (1974). *J. Appl. Cryst.* **7**, 593–598.

Beckmann, F., Bonse, U., Busch, F. & Gunnewig, O. (1997). *J. Comput. Assist. Tomogr.* **21**, 539–553.

Bonse, U. & Busch, F. (1996). *Prog. Biophys. Mol. Biol.* **65** 133–169.

Bonse, U. & Hart, M. (1965). *Appl. Phys. Lett.* **6**, 155–156.

Hart, M. (1975). *Proc. R. Soc. London Ser. A*, **346**, 1–22.

Momose, A. (1995). *Nucl. Instrum. Methods*, A**352**, 622–628.

Momose, A. & Fukuda, J. (1995). *Med. Phys.* **22**, 375–379.

Momose, A., Takeda, T. & Itai, Y. (1995). *Rev. Sci. Instrum.* **66**, 1434–1436.

Momose, A., Takeda, T. & Itai, Y. (1997). *Proc. SPIE*, **3149**, 120–129.

Momose, A., Takeda, T., Itai, Y. & Hirano, K. (1996*a*). *Proc. SPIE*, **2708**, 674–684.

Momose, A., Takeda, T., Itai, Y. & Hirano, K. (1996*b*). *Nature (London) Medicine*, **2**, 473–475.

Momose, A., Takeda, T., Itai, Y. & Hirano K. (1998). *X-ray Microscopy and Spectromicroscopy*, edited by J. Thieme, G. Schmahl, E. Umbach & D. Rudolph. Heidelberg: Springer-Verlag. In the press.

Momose, A., Takeda, T., Itai, Y., Yoneyama, A. & Hirano, K. (1998). *J. Synchrotron Rad.* **5**, 309–314.

Momose, A., Yoneyama, A. & Hirano, K. (1997). *J. Synchrotron Rad.* **4**, 311–312.

Suzuki, Y., Hayakawa, K., Usami, K., Hirano, T. & Endoh, T. (1989). *Rev. Sci. Instrum.* **60**, 2299–2302.

Takeda, T., Itai, Y., Hyodo, K., Ando, M., Akatsuka, T. & Uyama, C. (1998). *J. Synchrotron Rad.* **5**, 326–332.

Takeda, T., Momose, A., Itai, Y., Wu, J. & Hirano, K. (1995). *Acad. Radiol.* **2**, 799–803.